Nuclear Excitation by Electron Capture in Excited Ions

Simone Gargiulo,* Ivan Madan, and Fabrizio Carbone†
Institute of Physics (IPhys), Laboratory for Ultrafast Microscopy and Electron Scattering (LUMES), École Polytechnique Fédérale de Lausanne (EPFL), Lausanne 1015 CH, Switzerland

(Received 21 October 2020; revised 10 November 2021; accepted 4 April 2022; published 27 May 2022)

A nuclear excitation following the capture of an electron in an empty orbital has been recently observed for the first time. So far, the evaluation of the cross section of the process has been carried out widely using the assumption that the ion is in its electronic ground state prior to the capture. We show that by lifting this restriction new capture channels emerge resulting in a boost of more than three orders of magnitude to the electron capture resonance strength.

DOI: 10.1103/PhysRevLett.128.212502

Innovative technologies for harvesting and long-duration storing of energy are currently highly desired [1,2]. In this context, isomers are particularly attractive as they provide the potential for on-demand clean energy release combined with reliability, compactness, high stored energy density, and the ability to operate in extreme environment. The achievement of a controlled and efficient extraction of the isomeric energy has been a milestone for decades and is recently attracting growing attention [3–10]. In particular, recently demonstrated Nuclear Excitation by Electron Capture (NEEC) [11] could possibly offer gains in terms of control, as the electron switch of the process can be manipulated by means of electron optics and wave function engineering [10,12].

NEEC is a process in which the capture of a free or target electron by an ion results in the resonant excitation of a nucleus. The kinetic energy of the free electron E_r needs to equal the difference between the nuclear transition energy, E_n, and the atomic binding energy released through electron capture, E_b (i.e., $E_r = E_n - E_b$). The first isomer depletion induced by electron capture was recorded in a beam-based setup in 2018 [11], albeit the strength of the detected signal is unexplained by state-of-the-art theory [13], presenting a discrepancy of about nine orders of magnitude. Till today, NEEC is an object of a live debate [14–16].

Until this Letter, the NEEC process has been considered only in ions which are in their electronic ground states (ground state assumption, GSA) [17–20], in ground state ions with a single inner-shell hole created by x rays [21] or considering a statistical approach for electronic populations in an average atom model [22–24]. In this Letter, we examine the role of excited electronic configurations without any restrictions on the initial levels population. While the GSA allows for a straightforward account of the capture channels, it is too restrictive to unequivocally represent the real conditions taking place in out of equilibrium scenarios. In fact, it has been shown that, for a given charge state q, the ground state configuration usually is not the most probable [25]. It is therefore important to evaluate the cross sections of nuclear processes for a wider range of electronic configurations.

The GSA rules out the capture in the innermost shells for partially filled ions. For example, one can have K capture till two electrons fill the $1s$ orbital. However, even for fully ionized nuclei, NEEC into K shell may be forbidden if the energy released through a K capture (E_b^K) exceeds the nuclear transition energy (i.e., $E_r < 0$). Therefore, for such nuclei, under the GSA, NEEC with capture in the K shell is never possible. These channels can be re-enabled if sufficient screening is provided by an out of equilibrium electronic configuration, as we show for the example of ^{73}Ge.

In Fig. 1 we compare both the conventional and our approach. In Fig. 1(a) NEEC takes place in an ion under the GSA. A variant of NEEC—i.e., NEEC followed by a fast x-ray emission (NEECX)—considers the capture of the electron in a higher energy electronic shell while the ion is still in its electronic ground state, a situation in which the

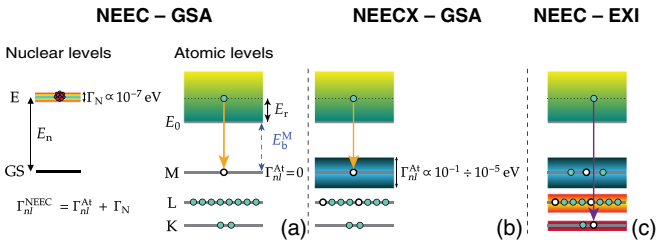

FIG. 1. Atomic configurations in case of electron capture: conventionally, the ion is considered to be in its nuclear and electronic ground states, while the capture either leaves the ion in the electronic ground state (a) referred to as NEEC, or brings it in an electronic excited state (b), referred to as NEECX. In (c), electrons can be distributed all over K, L, and M shells. Γ represents the width of the atomic (Γ_{nl}^{At}) and nuclear (Γ_N) transitions. For atomic ground states $\Gamma_{nl}^{At} = 0$, while for excited configurations $\Gamma_{nl}^{At} \gg \Gamma_N$.

GSA still holds [17,26], see Fig. 1(b). Instead, Fig. 1(c) represents the case in which the GSA does not hold: here, NEEC can occur even in excited ions (NEEC-EXI) and the consequences of such a scenario are discussed below.

The integrated NEEC cross section, called resonance strength S_{NEEC}, can be expressed as [19,27–31]:

$$S_{\mathrm{NEEC}}^{q,\alpha_r} = \int dE \frac{\lambda_e^2}{2} \hbar Y_{\mathrm{NEEC}}^{q,\alpha_r}(E) L_r(E - E_r), \qquad (1)$$

where λ_e is the electron wavelength and L_r is a Lorentzian function centered at the resonance energy of the free electron E_r. The width of such Lorentzian is given by the combination of both atomic configuration and nuclear level, $\Gamma_{nl}^{\mathrm{NEEC}} = \Gamma_{nl}^{\mathrm{At}} + \Gamma_N$. $Y_{\mathrm{NEEC}}^{q,\alpha_r}$ is the microscopic NEEC rate that depends on the final electronic configuration (α_r) and on the ion charge state q prior to the electron capture. Under the GSA, the initial electronic configuration (α_0) is uniquely defined by the charge state q and the number of available channels for capture in a particular subshell nl_j is strongly limited. By contrast, in NEEC-EXI the rate $Y_{\mathrm{NEEC}}^{q,\alpha_r}$ also depends on α_0, thus it has to be expressed as $Y_{\mathrm{NEEC}}^{q,\alpha_0,\alpha_r}$.

In NEEC-EXI, for a given charge state q, electrons are assigned to a particular shell from the innermost to the outermost (K, L, and M) encompassing all possible combinations. All these states are used as initial configurations α_0. In case the electron involved in the capture breaks the orbital angular momentum coupling in the initial atomic configuration α_0, the expression of the NEEC resonance strength in Eq. (1) is further complicated by an additional coefficient Λ, expressing the recoupling probability between the initial (α_0) and final electronic configurations (α_r) [32–37]:

$$S_{\mathrm{NEEC}}^{q,\alpha_0,\alpha_r} = \Lambda \int dE \frac{\lambda_e^2}{2} \hbar Y_{\mathrm{NEEC}}^{q,\alpha_0,\alpha_r}(E) L_r(E - E_r). \qquad (2)$$

In this Letter, the recoupling schemes for ions with up to four electrons filling the orbitals have been considered. Further details about the expression of Λ and electron recoupling are given in Supplemental Material [38]. The microscopic NEEC rate Y_{NEEC} is related to the process of internal conversion by time reversal. Using the principle of detailed balance [30], Y_{NEEC} can be expressed as a function of the internal conversion coefficients (ICCs) α_{IC}.

The determination of the ICCs for ions requires the knowledge of the electronic configuration and of the bound and free electron wave functions. In first approximation, ICCs for ions can be estimated from those of neutral atoms applying a scaling procedure, which relates ICC with the binding energy and occupancy of a specific subshell [20,22,39–42]. In this case, ICCs for neutral atoms are theoretically computed using the frozen orbital approximation based on the Dirac-Fock calculations [43]. Albeit ICCs for neutral atoms have been shown to have less than 1% uncertainty compared to experimental data [43–45], no detailed uncertainty analysis has been performed on ions for this scaling procedure.

For this reason, we compute Y_{NEEC} of selected channels also with the more advanced theory presented in Ref. [46], based on Feshbach projection operator formalism and compare these results with the ones obtained from the ICCs scaling procedure. Binding energies for a specific subshell and wave functions for a specific atomic configuration are computed using FAC [47]. FAC is a fully relativistic atomic code taking configuration interaction into account. Accuracy for the computed energy levels is assessed to be in the order of few electron volts [48].

Applying the GSA to the ^{73}Ge nuclear transition of $E_n = 13.2845$ KeV between the $9/2^+$ ground and the $5/2^+$ first excited states provides 47 L and M channels for $q = [29+, 32+]$, shown in Fig. 2(a) and tabulated in Supplemental Material [38]. Here, the K shell is energetically forbidden and L channels are the innermost available. The GSA allows for a drastic reduction of computational effort, as by lifting it, a total of 32 723 capture channels can be found in the same charge state range for L and M shells. Moreover, upon filling the orbitals, the electron screening lowers the binding energy of the K shell. Once E_b^K becomes smaller than E_n, NEEC into the K shell is possible. For ^{73}Ge this condition is met for $q = 29+$, for which 100 K-capture channels have been unveiled, as shown in Fig. 2(b). Most of these K channels (78) are characterized by an initial electronic configuration α_0 of the type $1s^1\, 2nl_j^1\, 3nl_j^1$ and occur in the energy range $E_r = [0, 38.8]$ eV, while for the remaining ones α_0 is $1s^1\, 2nl_j^2$, and $E_r = [48.2, 144.6]$ eV. All these K channels have one electron in the K shell prior to the electron capture: in fact, K captures with $\alpha_0 = \{2nl_j^3\}$ are still forbidden, since E_b^K is larger than E_n by about 200 eV at $q = 29+$. Resonance strengths for higher charge states are shown in Supplemental Material [38]. For L and M channels the widths of the atomic configurations $\Gamma_{nl}^{\mathrm{At}}$ is much smaller than the resonance energy E_r and Y_{NEEC} can be moved out of the integral in Eq. (2). In the case of K channels instead $\Gamma_{nl}^{\mathrm{At}} \approx E_r$ and the integral of Y_{NEEC} has to be performed. The widths for the atomic configurations leading to a K capture have been calculated using the XATOM code [49–51]. Notably, the higher number of channels identified in NEEC-EXI is not only due to the several initial configurations considered, but also to the increase of the capture channels available for a single excited configuration α_0 compared to the ground state counterpart. The reason is that excited configurations can have a larger number of open shells, thus the number of final configurations that can be generated are generally more numerous due to the higher number of combinations possible for the electron couplings.

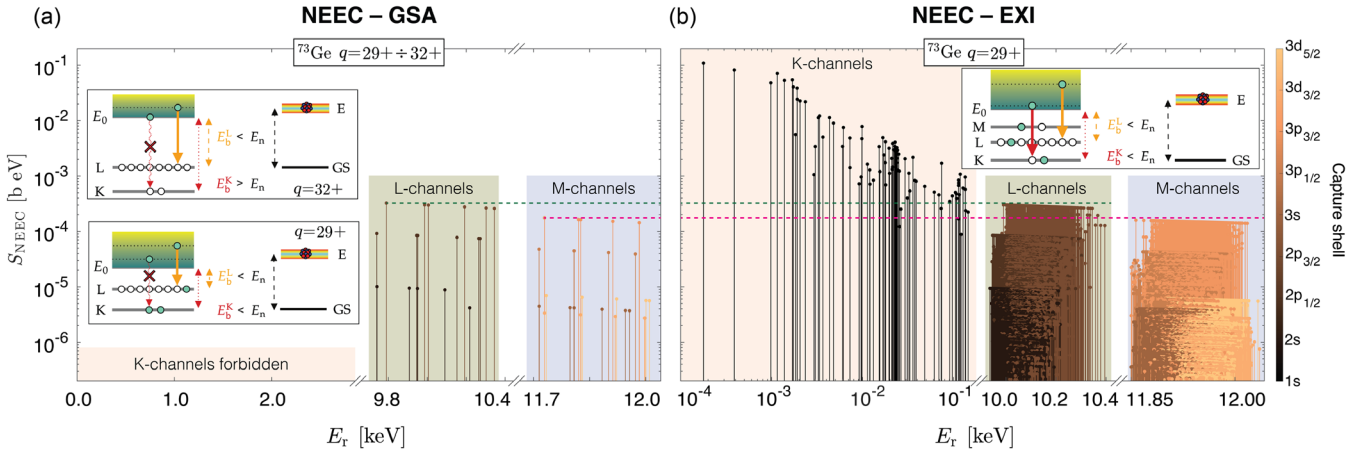

FIG. 2. (a) Resonance strengths for capture in the L shell (green box) and M shell (blue box) in case of ^{73}Ge with $q = [29+, 32+]$. NEEC in the K shell is energetically forbidden (pink box), since for high charge states the binding energy released for a K capture is bigger than the nuclear transition ($E_b^K > E_n$). For $q = 29 + E_b^K < E_n$, however the K shell is completely filled and capture cannot occur (insets). (b) Resonance strengths for ^{73}Ge in case all the possible combinations of initial and final electronic configurations are taken into account, for $q = 29+$. Each resonant channel is represented by a solid line, with its colors indicating the capture orbital. The horizontal green and magenta lines indicate the highest S_{NEEC}, under GSA, for L and M shells—occurring at $[q, \alpha_r] = [32+, 2p_{3/2}]$ and $[q, \alpha_r] = [32+, 3p_{3/2}]$—respectively.

Figure 2 compares the resonance strengths of the newly opened K channels with the L and M channels for NEEC-GSA and NEEC-EXI. Here, only shells up to the M have been considered, since α_0 with electrons in higher shells do not provide sufficient screening for a K capture at $q = 29+$. Selected channels are reported in Table I and, when possible, are compared with those evaluated with the GSA procedure for which Eq. (2) reduces to Eq. (1), since $\Lambda = 1$, and results coincide. Results for NEEC-EXI have been also evaluated using the wave function formalism (indicated as WF) and reported in Table I. The maximum value obtained in this case is of 5.18×10^{-1} beV. This allows us to comment on the accuracy of the ICC scaling procedure. Although the resonance strength obtained for a specific channel can be inaccurate by one order of magnitude, the ICC scaling reproduces the overall trend and the higher cross-section values in the case of NEEC-EXI. Furthermore, it allows us to have an easy estimate of the order of magnitude of the NEEC cross section in different experimental scenarios.

It is worth mentioning that the maximum value obtainable for the resonance strength with and without GSA differs by more than 3 orders of magnitude in the interval $q = [29+, 32+]$, due to the presence of the K channels. The highest values of the S_{NEEC} in the L and M shells instead are comparable between the two cases. There are two main factors defining the final S_{NEEC} value for a given character of the nuclear transition and E_n: (i) the resonance energy of the capture channel and (ii) the value of the microscopic NEEC rate $Y_{\mathrm{NEEC}}^{q,\alpha_0,\alpha_r}$. (i) Because of the resonant nature of the NEEC process, S_{NEEC} increases dramatically when the energy released through electron capture nearly matches the nuclear transition. (ii) $Y_{\mathrm{NEEC}}^{q,\alpha_0,\alpha_r}$ depends on the overlap between the bound and free electron wave functions. In the case of ^{73}Ge, the enhancement found for the K shell, compared to the highest value obtained under the GSA occurring for an $L3$ subshell, is due to an increase of the electron wavelength, since $Y_{\mathrm{NEEC}}^{q,\mathrm{K}} \leq Y_{\mathrm{NEEC}}^{q,\mathrm{L3}}$.

It is thus important to comment on the accuracy of the calculated energy levels. In Supplemental Material [38], we compare the 38 energy levels available for Ge, obtained from the NIST website [52], and the same reproduced by FAC. The results show a good agreement with discrepancies between these levels usually smaller than 1 eV and in all cases comparable with the accuracy reported for the $E2$ nuclear transition of ^{73}Ge. Although the S_{NEEC} values of the nearly resonant energy levels are affected by the accuracy of FAC, 27 K channels are present in the range $E_r = [0, 10]$ eV and 18 still forbidden in the range $E_r = [-10, 0]$ eV. Thus, a shift of few eV does not affect our conclusions. Similar screening effect on K channels can be found in other isotopes as ^{98}Tc and ^{125}Te. In the latter case, contrary to what happens for ^{73}Ge, a further increase of S_{NEEC} is expected due to a higher value of $\alpha_{\mathrm{IC}}^{\mathrm{q=0,K}}$ compared to $\alpha_{\mathrm{IC}}^{q=0,\mathrm{L}i}$, with $i \in \{1, 2, 3\}$.

An increase of the resonance strength is particularly valuable when NEEC is compared to competitive processes, such as the direct photoexcitation (DP) in the laser-generated plasma scenario [19,22,24,53]. Here, the discrimination of the two processes relies on the total number of excited nuclei, proportional to the corresponding photon or electron flux in plasma and the corresponding resonance strengths. In a tabletop laser based setup, the photon flux can exceed the electron flux by several orders of magnitude [19,38,54,55]. This might hinder the observation of NEEC even for such

TABLE I. Resonance strengths for ^{73}Ge in case of NEEC-EXI considering both the ICCs scaling procedure and the wave function (WF) formalism. For a given final electronic state (α_r) all the relative parent configurations α_0, that through electron capture can lead to it, are taken into consideration. Resonance energies are intended as $E_r = E_n - E_b$. When possible, a comparison with the conventional derivation (GSA) is also presented. Bold the subshell nl_j in which the capture occurs.

	^{73}Ge			NEEC GSA	NEEC-EXI	
q	Initial configuration (α_0)	Final configuration (α_r)	E_r (eV)	S_{NEEC} (b eV)	S_{NEEC} (b eV)	
				ICCs scaling	ICCs scaling	WF
32+	$\cdots$	$\mathbf{2p^1_{3/2}}$	9.79×10^3	3.26×10^{-4}	3.26×10^{-4}	1.25×10^{-4}
32+	$\cdots$	$\mathbf{2p^1_{1/2}}$	9.74×10^3	9.21×10^{-5}	9.21×10^{-5}	6.76×10^{-5}
31+	$1s^1$	$1s^1\,\mathbf{2s^1}$	9.91×10^3	9.49×10^{-6}	9.49×10^{-6}	8.37×10^{-6}
31+	$3d^1_{3/2}$	$\mathbf{2p^1_{1/2}}\,3d^1_{3/2}$	9.82×10^3	Not allowed	8.92×10^{-5}	6.56×10^{-5}
30+	$1s^2$	$1s^2\,\mathbf{2s^1}$	10.09×10^3	8.82×10^{-6}	8.82×10^{-6}	7.47×10^{-6}
30+	$3d^1_{3/2}\,3d^1_{5/2}$	$\mathbf{2p^1_{3/2}}\,3d^1_{3/2}\,3d^1_{5/2}$	9.96×10^3	Not allowed	2.67×10^{-4}	1.05×10^{-4}
29+	$1s^2\,2s^1$	$1s^2\,2s^1\,\mathbf{2p^1_{1/2}}$	10.26×10^3	7.46×10^{-5}	7.46×10^{-5}	5.19×10^{-5}
29+	$3p^1_{3/2}\,3d^1_{3/2}\,3d^1_{5/2}$	$\mathbf{2p^1_{3/2}}\,3p^1_{3/2}\,3d^1_{3/2}\,3d^1_{5/2}$	10.06×10^3	Not allowed	6.30×10^{-5}	2.53×10^{-5}
29+	$3p^1_{3/2}\,3d^1_{3/2}\,3d^1_{5/2}$	$\mathbf{2p^1_{1/2}}\,3p^1_{3/2}\,3d^1_{3/2}\,3d^1_{5/2}$	10.03×10^3	Not allowed	7.18×10^{-5}	5.58×10^{-5}
29+	$1s^1\,2p^1_{1/2}\,2p^1_{3/2}$	$\mathbf{1s^2}\,2p^1_{1/2}\,2p^1_{3/2}$	144.62	Not allowed	2.23×10^{-4}	9.40×10^{-4}
29+	$1s^1\,2s^2$	$\mathbf{1s^2}\,2s^2$	73.87	Not allowed	1.71×10^{-3}	7.28×10^{-3}
29+	$1s^1\,2s^1\,3d^1_{5/2}$	$\mathbf{1s^2}\,2s^1\,3d^1_{5/2}$	4.32	Not allowed	1.14×10^{-2}	4.94×10^{-2}
29+	$1s^1\,2s^1\,3p^1_{1/2}$	$\mathbf{1s^2}\,2s^1\,3p^1_{1/2}$	1.15	Not allowed	7.14×10^{-2}	3.10×10^{-1}
29+	$1s^1\,2p^1_{3/2}\,3d^1_{3/2}$	$\mathbf{1s^2}\,2p^1_{3/2}\,3d^1_{3/2}$	0.98	Not allowed	4.82×10^{-2}	2.32×10^{-1}
29+	$1s^1\,2p^1_{3/2}\,3d^1_{3/2}$	$\mathbf{1s^2}\,2p^1_{3/2}\,3d^1_{3/2}$	0.39	Not allowed	8.25×10^{-2}	3.61×10^{-1}
29+	$1s^1\,2s^1\,3p^1_{3/2}$	$\mathbf{1s^2}\,2s^1\,3p^1_{3/2}$	0.18	Not allowed	1.09×10^{-1}	5.18×10^{-1}

promising nuclei as ^{73}Ge, for which the DP resonance strength of the $E2$ transition is $S_\gamma = 1.93 \times 10^{-6}$ beV, significantly smaller than the highest $S_{\mathrm{NEEC}} = 1.25 \times 10^{-4}$ beV, obtained under the GSA. Conversely, lifting the GSA allows for the appearance of capture channels in the K shell characterized by higher S_{NEEC} values. This is particularly relevant if an additional external electron source is considered. For a few kilo electron volts temperature plasma, the flux of electrons at low energies corresponding to K channels is small and of the order of 10^{21} cm^{-2} s^{-1} eV^{-1}. Under this condition, the use of an external adjustable electron source [38,56] could allow us to overcome the deficit in the electron flux and decouple it from other plasma parameters. We point out here that the determination of the total number of excited nuclei would require the knowledge of the survival time of each atomic configuration in a specific experimental scenario. To the best of our knowledge, this level of detail is not available with current simulation tools.

In out-of-equilibrium scenarios, excited electronic configurations might be more likely to occur [25] and the same can hold true for the ^{93}Mo isomer depletion of Ref. [11]. Indeed, during the entire impact with the carbon target, ^{93}Mo ions are considered to be in their electronic ground state. This makes the contributions from the L shell negligible, although the resonance strengths for the L channels are the highest [13]. This happens because the ion fraction in the charge state $q \geq 33+$ required for L-shell vacancies is extremely small when the resonant conditions are met. Recently, a study considering the Compton profile of target electrons [16] shed new light on the importance of these L channels, shifting upward by several orders of magnitude their theoretical contribution to the partial NEEC probability. In particular, this study shows that the L channels are no longer insignificant and their contribution is comparable with that of higher shells. Nevertheless, the total NEEC probability, accounting for charge state distribution and available vacancies, only slightly increases leaving the current discrepancy mostly unaltered. Indeed, under the GSA, the L channels are not available at low projectile energies, where they give most of their contribution [16]. If instead electronic excitations would make L vacancies survive even for $q < 33+$, NEEC-EXI might reveal new capture L channels even at low ion beam energy. The presence of these new channels, combined with their persistence over an energy continuum [16], might possibly reduce the discrepancy between the experimental observation and theoretical predictions.

In NEEC scenarios only the energy matching between free electrons, bound states, and nuclear transitions has been historically addressed. Since selection rules for NEEC require $j_c - L \leq j_f \leq j_c + L$, where L is the multipolarity of the transition, in Ref. [12] we proposed that angular

momentum matching could have given the possibility to select and enhance the capture in the innermost shells, by tuning the individual orbital angular momentum (OAM) $l\hbar$ of an external free electron beam [57–60], using phase plates or chiral plasmons [61–63]. When using such OAM-carrying electrons (called vortex beam) the expressions used for Y_{NEEC} do not hold in the same form, thus leading to different values for the S_{NEEC}. Recently, this has been shown in detail to be a way to increase the NEEC cross section by several orders of magnitude [64]. The combination of this additional degree of freedom with the presence of excited electronic configurations could open a possibility to further boost the NEEC rate in a plasma scenario by providing specific atomic vacancies and pulsed vortex electrons at the resonant energy to selectively choose the capture in the desired shell.

In conclusion, we have shown that the common assumption that NEEC takes place in an ion in its electronic ground state significantly restricts the available channels. By lifting this condition, we have shown that in ^{73}Ge the NEEC resonance strengths gain more than three orders of magnitude. Thus, this work heralds the possibility of a reevaluation of the isotopes prematurely disregarded and those already in use in out-of equilibrium scenarios. These findings could open a new route for an externally controlled nuclear excitation by providing excited configurations and resonant engineered electrons from an external source, thus selecting the promising channels for on-demand isomer depletion. In particular, the inclusion of excited electronic configurations in the theoretical model describing the first NEEC observation in ^{93}Mo, as here done for ^{73}Ge, could reduce the discrepancy between the actual theoretical predictions and experimental observation.

The LUMES laboratory acknowledges support from the NCCR MUST and Google Inc. The authors would like to thank G. M. Vanacore, C. J. Chiara, and J. J. Carroll for insightful discussions. The authors are indebted to A. Pálffy and Y. Wu for their useful feedback and for providing details on the derivation of the theory presented in Ref. [46].

*simone.gargiulo@epfl.ch
†fabrizio.carbone@epfl.ch

[1] R. Koningstein and D. Fork, IEEE Spectrum **51**, 30 (2014).
[2] N. A. Sepulveda, J. D. Jenkins, A. Edington, D. S. Mallapragada, and R. K. Lester, Nat. Energy **6**, 506 (2021).
[3] P. Walker and G. Dracoulis, Nature (London) **399**, 35 (1999).
[4] C. B. Collins, F. Davanloo, M. C. Iosif, R. Dussart, J. M. Hicks, S. A. Karamian, C. A. Ur, I. I. Popescu, V. I. Kirischuk, J. J. Carroll, H. E. Roberts, P. McDaniel, and C. E. Crist, Phys. Rev. Lett. **82**, 695 (1999).
[5] M. Litz and G. Merkel, Controlled extraction of energy from nuclear isomers, Technical Report No. ADA433348, Army Research Laboratory, Adelphi, MD, 2004.
[6] C. B. Collins, N. C. Zoita, F. Davanloo, S. Emura, Y. Yoda, T. Uruga, B. Patterson, B. Schmitt, J. M. Pouvesle, I. Popescu *et al.*, Radiat. Phys. Chem. **71**, 619 (2004).
[7] A. Aprahamian and Y. Sun, Nat. Phys. **1**, 81 (2005).
[8] A. Y. Dzyublik, Nucl. Phys. At. Energy **14**, 11 (2013).
[9] J. Carroll, M. Litz, K. Netherton, S. Henriquez, N. Pereira, D. Burns, and S. Karamian, in *AIP Conference Proceedings* (American Institute of Physics, Melville, 2013), Vol. 1525, pp. 586–594.
[10] G. M. Vanacore, I. Madan, G. Berruto, K. Wang, E. Pomarico, R. Lamb, D. McGrouther, I. Kaminer, B. Barwick, F. J. G. de Abajo, and F. Carbone, Nat. Commun. **9**, 2694 (2018).
[11] C. J. Chiara, J. J. Carroll, M. P. Carpenter, J. P. Greene, D. J. Hartley, R. V. Janssens, G. J. Lane, J. C. Marsh, D. A. Matters, M. Polasik, J. Rzadkiewicz, D. Seweryniak, S. Zhu, S. Bottoni, and A. B. Hayes, Nature (London) **554**, 216 (2018).
[12] I. Madan, G. M. Vanacore, S. Gargiulo, T. Lagrange, and F. Carbone, Appl. Phys. Lett. **116**, 230502 (2020).
[13] Y. Wu, C. H. Keitel, and A. Pálffy, Phys. Rev. Lett. **122**, 212501 (2019).
[14] S. Guo, Y. Fang, X. Zhou, and C. Petrache, Nature (London) **594**, E1 (2021).
[15] C. Chiara, J. Carroll, M. Carpenter, J. Greene, D. Hartley, R. Janssens, G. Lane, J. Marsh, D. Matters, M. Polasik *et al.*, Nature (London) **594**, E3 (2021).
[16] J. Rzadkiewicz, M. Polasik, K. Słabkowska, L. Syrocki, J. J. Carroll, and C. J. Chiara, Phys. Rev. Lett. **127**, 042501 (2021).
[17] A. Pálffy, Z. Harman, C. Kozhuharov, C. Brandau, C. H. Keitel, W. Scheid, and T. Stöhlker, Phys. Lett. B **661**, 330 (2008).
[18] Y. Wu, J. Gunst, C. H. Keitel, and A. Pálffy, Phys. Rev. Lett. **120**, 052504 (2018).
[19] J. Gunst, Y. Wu, C. H. Keitel, and A. Pálffy, Phys. Rev. E **97**, 063205 (2018).
[20] J. Rzadkiewicz, M. Polasik, K. Słabkowska, L. Syrocki, E. Wéder, J. J. Carroll, and C. J. Chiara, Phys. Rev. C **99**, 044309 (2019).
[21] Y. Wu, C. H. Keitel, and A. Pálffy, Phys. Rev. A **100**, 063420 (2019).
[22] G. Gosselin and P. Morel, Phys. Rev. C **70**, 064603 (2004).
[23] G. D. Doolen, Phys. Rev. Lett. **40**, 1695 (1978).
[24] G. D. Doolen, Phys. Rev. C **18**, 2547 (1978).
[25] S.-K. Son, R. Thiele, Z. Jurek, B. Ziaja, and R. Santra, Phys. Rev. X **4**, 031004 (2014).
[26] M. Polasik, K. Słabkowska, J. J. Carroll, C. J. Chiara, Ł. Syrocki, E. Weder, and J. Rzadkiewicz, Phys. Rev. C **95**, 034312 (2017).
[27] S. S. Wong, *Introductory Nuclear Physics* (John Wiley & Sons, New York, 2008).
[28] A. Zadernovsky and J. Carroll, Hyperfine Interact. **143**, 153 (2002).
[29] M. R. Harston and J. F. Chemin, Phys. Rev. C **59**, 2462 (1999).
[30] J. Oxenius, *Springer Series in Electrophysics* (Springer Science & Business Media, Berlin, 1986).
[31] A. Pálffy, W. Scheid, and Z. Harman, Phys. Rev. A **73**, 012715 (2006).

[32] P. V. Bilous, G. A. Kazakov, I. D. Moore, T. Schumm, and A. Pálffy, Phys. Rev. A **95**, 032503 (2017).

[33] A. P. Yutsis, V. Vanagas, and I. B. Levinson, *Mathematical Apparatus of the Theory of Angular Momentum* (Israel Program for Scientific Translations, Jerusalem, 1962).

[34] L. C. Biedenharn and J. D. Louck, *The Racah-Wigner Algebra in Quantum Theory* (Addison-Wesley, Reading, MA, 1981).

[35] V. Aquilanti, A. C. P. Bitencourt, C. D. S. Ferreira, A. Marzuoli, and M. Ragni, Phys. Scr. **78**, 058103 (2008).

[36] V. Fack, S. N. Pitre, and J. Van der Jeugt, Comput. Phys. Commun. **86**, 105 (1995).

[37] V. Fack, S. Lievens, and J. Van Der Jeugt, Comput. Phys. Commun. **119**, 99 (1999).

[38] See Supplemental Material at http://link.aps.org/supplemental/10.1103/PhysRevLett.128.212502 for further details on the ICC scaling procedure and wave function formalism, the computed values in case of GSA for ^{73}Ge, recoupling coefficients, accuracy of the FAC calculations, the 3D plot showing S_{NEEC} for NEEC-EXI in ^{73}Ge with $q = [29+, 32+]$, and NEEC-GSA in the laser-plasma scenario (2021).

[39] M. Rysavý and O. Dragoun, J. Phys. G **26**, 1859 (2000).

[40] F. Larkins, At. Data Nucl. Data Tables **20**, 311 (1977).

[41] K. D. Sevier, At. Data Nucl. Data Tables **24**, 323 (1979).

[42] J. Kantele, Nucl. Instrum. Methods Phys. Res., Sect. A **275**, 149 (1989).

[43] T. Kibedi, T. Burrows, M. B. Trzhaskovskaya, P. M. Davidson, and C. W. Nestor, Jr., Nucl. Instrum. Methods Phys. Res., Sect. A **589**, 202 (2008).

[44] T. Kibédi, T. W. Burrows, M. B. Trzhaskovskaya, C. W. Nestor, Jr., and P. M. Davidson, Int. Conf. Nucl. Data Sci. Technol. 57 (2007).10.1051/ndata:07771

[45] S. Raman, C. W. Nestor, Jr., A. Ichihara, and M. B. Trzhaskovskaya, Phys. Rev. C **66**, 044312 (2002).

[46] A. Pálffy, Theory of nuclear excitation by electron capture for heavy ions, Ph.D. thesis, Justus-Liebig-Universität, 2006.

[47] M. F. Gu, Can. J. Phys. **86**, 675 (2008).

[48] G. Massacrier and M.-C. Artru, Astron. Astrophys. **538**, A52 (2012).

[49] Z. Jurek, S.-K. Son, B. Ziaja, and R. Santra, J. Appl. Crystallogr. **49**, 1048 (2016).

[50] S.-K. Son, L. Young, and R. Santra, Phys. Rev. A **83**, 033402 (2011).

[51] B. Murphy, T. Osipov, Z. Jurek, L. Fang, S.-K. Son, M. Mucke, J. Eland, V. Zhaunerchyk, R. Feifel, L. Avaldi *et al.*, Nat. Commun. **5**, 1 (2014).

[52] A. Kramida, Yu. Ralchenko, J. Reader, and NIST ASD Team, NIST Atomic Spectra Database (ver. 5.6.1) (2015), Available: https://physics.nist.gov/asd, National Institute of Standards and Technology, Gaithersburg, MD, 2018.

[53] J. F. Gunst, Mutual control of x-rays and nuclear transitions, Ph.D. thesis, Ruprecht-Karls-Universität Heidelberg, 2015.

[54] P. Gibbon and E. Förster, Plasma Phys. Controlled Fusion **38**, 769 (1996).

[55] H.-K. Chung, M. Chen, W. Morgan, Y. Ralchenko, and R. Lee, High Energy Density Phys. **1**, 3 (2005).

[56] D. Filippetto, P. Musumeci, M. Zolotorev, and G. Stupakov, Phys. Rev. ST Accel. Beams **17**, 024201 (2014).

[57] J. Verbeeck, H. Tian, and P. Schattschneider, Nature (London) **467**, 301 (2010).

[58] S. Lloyd, M. Babiker, G. Thirunavukkarasu, and J. Yuan, Rev. Mod. Phys. **89**, 035004 (2017).

[59] J. Verbeeck, A. Béché, K. Müller-Caspary, G. Guzzinati, M. A. Luong, and M. Den Hertog, Ultramicroscopy **190**, 58 (2018).

[60] G. M. Vanacore, I. Madan, and F. Carbone, Riv. Nuovo Cimento **43**, 567 (2020).

[61] K. Y. Bliokh, I. P. Ivanov, G. Guzzinati, L. Clark, R. Van Boxem, A. Béché, R. Juchtmans, M. A. Alonso, P. Schattschneider, F. Nori, and J. Verbeeck, Phys. Rep. **690**, 1 (2017).

[62] G. M. Vanacore, G. Berruto, I. Madan, E. Pomarico, P. Biagioni, R. J. Lamb, D. McGrouther, O. Reinhardt, I. Kaminer, B. Barwick, H. Larocque, V. Grillo, E. Karimi, F. J. García de Abajo, and F. Carbone, Nat. Mater. **18**, 573 (2019).

[63] V. Grillo, A. H. Tavabi, F. Venturi, H. Larocque, R. Balboni, G. C. Gazzadi, S. Frabboni, P.-H. Lu, E. Mafakheri, F. Bouchard *et al.*, Nat. Commun. **8**, 15536 (2017).

[64] Y. Wu, S. Gargiulo, F. Carbone, C. H. Keitel, and A. Pálffy, Phys. Rev. Lett. **128**, 162501 (2022).